Contact Networks Enhance Shear Thickening in Attractive Colloid-Polymer Mixtures

Nayoung Park, Vikram Rathee, Daniel L. Blair, and Jacinta C. Conrad

Phys. Rev. Lett. **122**, 228003 — Published 7 June 2019

DOI: 10.1103/PhysRevLett.122.228003

Contact networks enhance shear thickening in attractive colloid-polymer mixtures

Nayoung Park,[1] Vikram Rathee,[2, 3] Daniel L. Blair,[2, 3] and Jacinta C. Conrad[1, *]
[1] *Department of Chemical and Biomolecular Engineering*
University of Houston, Houston, TX 77204
[2] *Department of Physics*
Georgetown University, Washington, DC 20057
[3] *Institute for Soft Matter Synthesis and Metrology*
Georgetown University, Washington, DC 20057
(Dated: May 15, 2019)

Increased shear thinning arising due to strong attractive interactions between colloidal particles is thought to obscure shear thickening. Here, we demonstrate how moderate attractions, induced by adding a non-adsorbing polymer, can instead enhance shear thickening. We measure the rheology of colloidal suspensions at a constant particle volume fraction of $\phi = 0.40$ with dilute to weakly semi-dilute concentrations of three polyacrylamide depletants of different molecular weights. Suspensions containing large polymer exhibit increased shear thickening and positive first normal stress differences at high shear stress, and increased heterogeneous fluctuations in the boundary stress. These results are consistent with a friction-based model for shear thickening, suggesting that the presence of large, extended polymers induces the formation of near-spanning networks of interparticle contacts.

Dense suspensions of particles with repulsive interactions usually exhibit shear thickening, an increase in viscosity with shear rate $\dot{\gamma}$ [1]. In continuous shear thickening (CST), this increase is gradual and reverses upon decrease in $\dot{\gamma}$. Microscopic mechanisms underlying CST are vigorously debated, with studies highlighting both lubrication (hydrodynamic) [2–4] and friction (contact) [5–10] interactions. The sign of the first normal stress difference N_1 is used to distinguish the contributions from these interactions [10], with negative and positive N_1 corresponding to lubrication [11, 12] and friction [6, 13], respectively. Introducing additional interactions between the particles is thus expected to affect shear thickening.

Strong short-range interparticle attractions suppress shear thickening [14, 15]. In CST colloidal suspensions, this suppression was proposed to arise when the attractive thermodynamic contribution to viscosity overwhelmed that from hydrodynamic interactions [14]. Simulations of colloidal suspensions with both lubrication and contact interactions challenge this perspective, showing that contact is important even for CST: suspensions with weak interparticle attractions shear thickened, although sufficiently strong attractions still obscured thickening [16]. None of these studies, however, suggest that interparticle attractions (with possible exception of bridging attractions [17]) may enhance shear thickening.

Non-adsorbing polymers added to a colloidal suspension induce short-range depletion attractions, whose stresses can overwhelm thickening [14]. The polymer itself may also alter suspension rheology. In filled polymers, the elasticity of the polymer medium can dramatically affect N_1 [18–20], with increases in shear thickening attributed to particle-induced fluid stresses in elastic polymer solutions [21–23]. These studies, however, largely treat polymer solutions or melts as continuum fluids and do not consider effects arising from variation in polymer molecular weight or polymer-induced attractions between particles.

In this Letter, we show that polymer depletants added to colloidal suspensions can markedly enhance CST through formation of force-bearing contact networks, depending on polymer molecular weight. Suspensions containing large polymers exhibited a pronounced increase in shear thickening with polymer concentration at dilute to semi-dilute concentrations ($c/c^* \leq 1.3$) with an accompanying change in the sign of N_1. The elasticity (as deduced from N_1) of the background polymer solution was nearly independent of polymer size at these concentrations, indicating that differences in suspension rheology did not arise from changes in background elasticity. Analyzing the results with a friction-based model [5, 10, 24] and measuring boundary stress fluctuations [25], we show that the presence of large polymers increased the fraction of particles in contact, leading to positive N_1 and pronounced fluctuations in boundary stress. This effect arises when the sheared, extended polymer is large enough to be excluded from lubrication layers between particles. These results suggest that shear thickening can be enhanced or reduced via addition of non-adsorbing polymers of different molecular weight. This ability to tune shear thickening can be used to probe microscopic mechanisms driving shear thickening and to improve the efficiency of colloidal materials processing [1].

Poly(2,2,2-trifluoroethyl methacrylate-*co*-*tert*-butyl methacrylate) particles (D_H = 1500 nm (PDI 0.1), D_H = 1580 nm (PDI 0.06)) were synthesized [26] to be refractive index- and density-matched to 80 (w/w)% glycerol in water; 20 mM NaCl was added to partly screen electrostatic repulsions between particles. Depletion attractions between particles were induced by adding solutions of polyacrylamide in 80 (w/w)% glycerol/water [27] to particle suspensions, such that particle volume fraction $\phi = 0.40$ was constant throughout all samples. Three polyacrylamides of various weight-average molecular weight M_w and dispersity Đ were used as depletants: M_w = 185.7 kDa, Đ = 1.4, Polymer Source (hereafter, USP); M_w = 1.15 MDa, Đ = 1.8, PolySciTech (ULP); and M_w = 1.97 MDa, Đ = 21, Sigma-Aldrich (DP). The range of the attraction was $R_g/a \approx 0.03 - 0.07$, and the minimum in electrostatic + depletion energy ranged between $\mathcal{O}$(-1 kT) and $\mathcal{O}$(-10 kT). Suspensions were imaged on an inverted Leica microscope equipped with a VT-Eye confocal scanhead [27]. Measurements of viscosity η and N_1 were performed on a DHR-2 Rheometer (TA Instruments, New Castle, DE) with a 40 mm diameter, 2° hard-anodized aluminum cone, following established protocols [27][28]. Normal stress differences from raw axial force were corrected for inertia [29] and initial value measured at the lowest shear rate $N_{1,0}$. The particle Reynolds number [30] $\mathrm{Re}_p \leq 8 \times 10^{-6}$ indicated that inertial effects on particles were negligible; the geometric Reynolds number [31] $\mathrm{Re} \leq 0.05$ indicated that secondary flows were minimal. The Péclet number $1 \times 10^1 \leq \mathrm{Pe} \leq 3 \times 10^5$ indicated that stresses arising from Brownian motion could be neglected.

In the absence of polymer, the $\phi = 0.40$ suspension exhibited weak CST at a critical shear stress of 30 Pa and $N_1 \leq 0$ at all accessible shear stresses σ (Fig. 1a,d), as expected for dense suspensions of nearly hard spheres [4, 10, 32]. Addition of USP at constant ϕ increased the low-shear viscosity of the suspensions and generated pronounced shear thinning for $\sigma \lesssim 5$ Pa. The shear-thinning exponent n ($\eta \sim \sigma^{-n}$) increased from 0.04 to 1.2 with increasing USP concentration, consistent with shear thinning arising from stronger attractions between particles (Fig. 2a) [33, 34]. As σ was further increased, the viscosity first reached a plateau and then increased slightly, again displaying weak CST. The shear thickening exponent $\beta = 0.1$ ($\eta \sim \sigma^{\beta}$) in the absence of polymer, and remained constant as USP concentration was increased up to $c/c^* = 1.2$ (Fig. 2b). Addition of USP did not markedly alter either shear thickening or N_1, indicating that CST arose from formation of hydroclusters. For USP solutions, $N_1 \geq 0$ at high σ in the absence of particles, as expected for polymer solutions, but ≤ 0 in the presence of particles. This result suggests that USP was incorporated in the lubrication layers between particles in hydroclusters, which dominate N_1.

Addition of ULP resulted in weaker shear thinning but stronger shear thickening at high σ (Fig. 1b), as indicated by an increase in β from 0.1 to 0.3. Stronger shear thickening was accompanied by a switch in the sign of N_1, from negative in hard spheres to positive in ULP, with magnitudes of N_1 a factor of 10 higher than those observed for nearly hard spheres (Fig. 1e). These strikingly different trends in η and N_1 were observed at same ϕ and c/c^* in USP and ULP samples, despite similar η and N_1 of the background polymer solutions [35] and nearly identical quiescent particle microstructures (Fig. 1d,e insets).

Suspensions containing DP, which had comparable number-average and weight-average molecular weights to USP and ULP, exhibited trends in η and N_1 analogous to those of suspensions with ULP. Shear-thinning exponents n of ULP and DP suspensions scaled identically as a function of c/c^*, and were smaller than n values obtained for suspensions containing USP. Shear thinning in attractive suspensions reflects breaking of bonds between clusters of particles [33, 34]; smaller n values observed for ULP and DP are consistent with weaker attractions induced (in equilibrium) by large polymers at fixed c/c^*. Likewise, β values were larger for suspensions containing ULP or DP than for those containing USP, although $\beta \leq 0.3$ indicated that all samples were in the CST regime. Further, ULP samples exhibited larger β values than DP samples. Together, these results suggest that the relatively high M_w of DP and ULP polymers generated the changes in shear thickening and N_1.

For CST driven by hydrodynamic interactions, β is expected to remain constant as the strength of attractions is increased [14], as observed in USP suspensions. In ULP and DP suspensions, however, β increased as c/c^* was increased. The increase in β and change in sign of N_1 (as compared to the hard-sphere suspension) observed as c/c^* was increased in ULP and DP samples are, instead, reminiscent of the signatures of contact networks of particles in dense, shear-thickening suspensions of hard spheres [10]. Inspired by a theoretical model [5] positing that discontinuous shear thickening emerges when frictional contacts form upon exceeding a critical stress, Ref. [10] postulated that the change in sign of N_1 from negative to positive signals the formation of an interconnected network of frictional contacts throughout the sample. Negative values of N_1, by contrast, reflect contacts between particles confined within hydroclusters held together by lubrication forces.

To test the hypothesis that contact networks drive the observed changes in rheology for suspensions containing large polymers, the friction-based model of Ref. [5] as modified in Ref. [10, 24] was fit to the shear-thickening portion of all viscosity curves. This model posits that the total relative viscosity η_r arises from the competition between two branches of viscosities, each of which diverges when the particles become jammed. In the lower stress branch, particles maintain lubrication layers such that the viscosity diverges at the close-packed ϕ_0. In the higher stress branch, particle surfaces make contact such that the viscosity diverges at a lower, friction-dependent

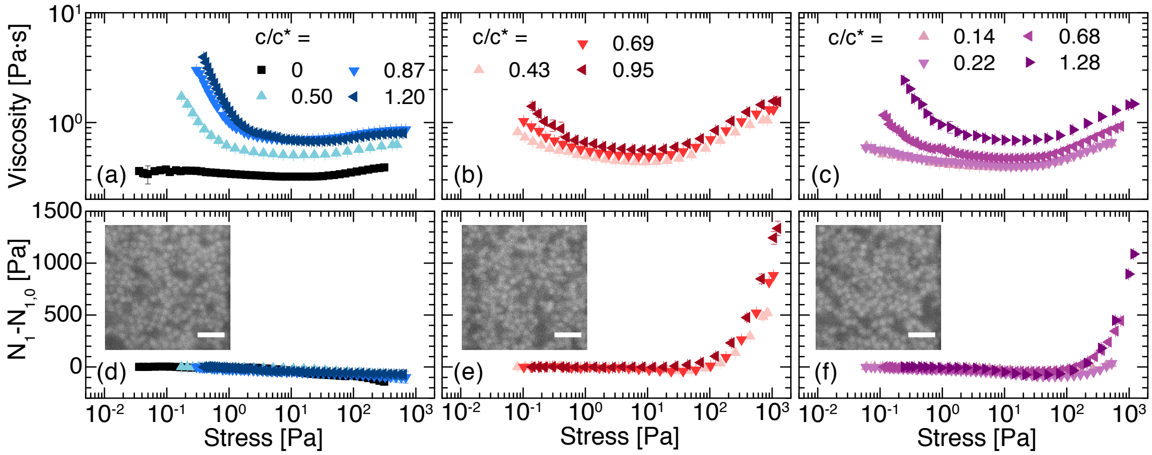

FIG. 1. (a-c) Viscosity and (d-f) corrected N_1 as a function of shear stress for $\phi = 0.40$ suspensions with various free-volume concentrations of polyacrylamide c/c^*, normalized by the overlap concentration c^*. Polymers (a,d) USP, (b,e) ULP, (c,f) DP. Insets: Micrographs of quiescent suspensions with $c/c^* =$ (d) 0.5 USP, (e) 0.7 ULP, and (f) 0.7 DP. Scale bars: 5 μm.

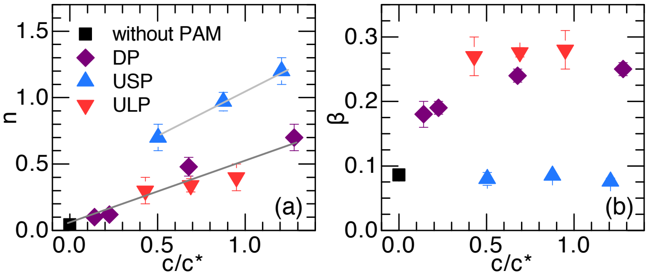

FIG. 2. Power-law (a) shear-thinning (n) and (b) shear-thickening (β) exponents as a function of normalized polyacrylamide (USP, ULP, DP) concentration in the free volume c/c^* for $\phi = 0.40$ suspensions. Gray lines are guides for the eye.

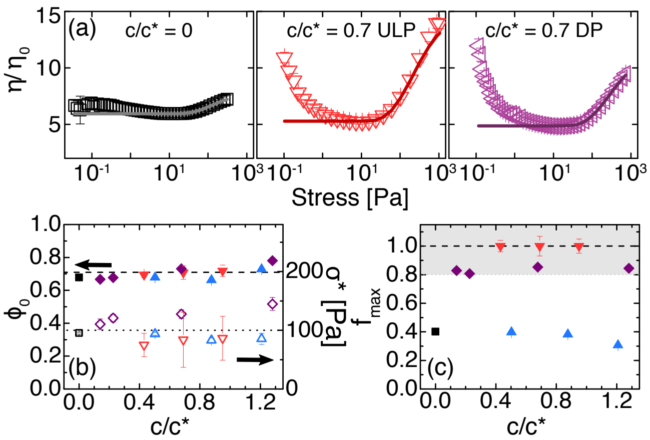

FIG. 3. (a) Relative viscosity as a function of stress, fit to Eq. 1 [5, 10] for representative suspensions without polymer, with normalized polyacrylamide concentration in the free volume $c/c^* = 0.7$ ULP, and with $c/c^* = 0.7$ DP. (b-c) Fit parameters extracted from Eq. 1 as a function of c/c^*. Dashed lines are guides for the eye at (b) $\phi_0 = 0.71$, $\sigma^* = 100$ Pa, (c) $f_{\max} = 1$. Samples in the shaded region ($f_{\max} > 0.8$) exhibited $N_1 > 0$.

volume fraction ϕ_m. The viscosity η_r is thus given by

$$\eta_r(\sigma, \phi) = \left(1 - \frac{\phi}{\phi_c(\sigma)}\right)^{-2}, \qquad (1)$$

where the critical volume fraction $\phi_c(\sigma) = f\phi_m + (1 - f)\phi_0$. The fraction of particles in contact $f(\sigma, \phi) = f_{\max}(\phi)e^{-\sigma^*/\sigma}$ [10] is a function of σ, critical stress for particles to overcome repulsive forces σ^*, and maximum fraction of particles in contact $f_{\max}$.

The friction-based model (Eq. 1) quantitatively fit the shear thickening in all samples (Fig. 3a) using fixed $\phi_m = 0.54$ [4] and variable ϕ_0, σ^*, and $f_{\max}$ [35]. The resulting $\phi_0 \approx 0.7$ and $\sigma^* \approx 100$ Pa were independent of c/c^* across all samples (USP, ULP, or DP) (Fig. 3b), and comparable to values ($\phi_0 = 0.71$ and $\sigma^* \approx 170$ Pa) reported for hard-sphere suspensions [10]. The near-constant ϕ_0, the close-packing fraction at which lubricated particles jam, is expected for particles of similar size and dispersity. The fact that σ^* obtained here is comparable to that for hard-sphere suspensions indicates that polymers do not alter the repulsive forces between particles that prevent contact.

Whereas ϕ_0 and σ^* were similar across all samples, $f_{\max}$ was notably larger in the presence of ULP and DP. We found $f_{\max} = 1$ for ULP suspensions and $f_{\max} \approx 0.8$ for DP (Fig. 3), but $f_{\max} \approx 0.4$ of USP samples was close to that of the hard-sphere sample. Both β and N_1 exhibited a pronounced increase when $f_{\max}$ approached 1 in samples containing large polymers. This increase is similar to the dramatic evolution of β and N_1 when $f_{\max} = 1$ in dense suspensions without polymers [10], and is consistent with the development of a space-spanning network of contacts.

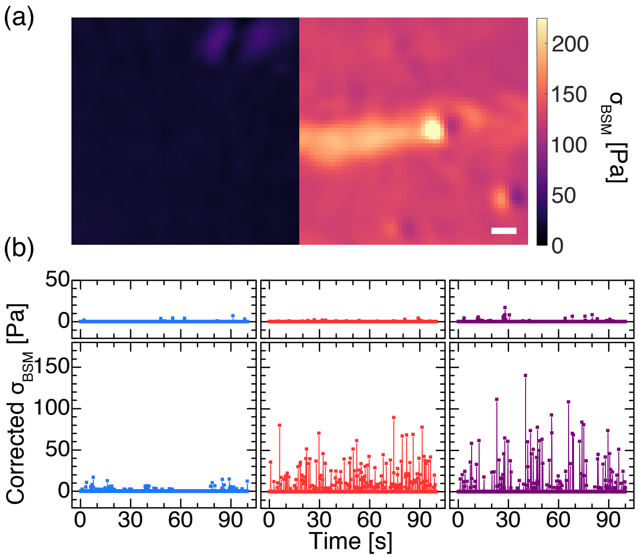

FIG. 4. (a) Examples of boundary stress (in units of Pa) with weak and strong heterogeneity events. Shared scale bar: 100 μm. (b) Average boundary stress as a function of measurement time while shearing at a rate of 100 s^{-1} (top row) and 500 s^{-1} (bottom row) for USP (first column), ULP (second column), and DP (third column) samples with $c/c^* = 0.7$.

As a second signature of contact network formation, dense suspensions of hard-sphere colloids exhibit pronounced heterogeneities in boundary stress, reflecting the separation into high-viscosity and low-viscosity fluid phases during CST [25]. Using boundary stress microscopy (BSM), Ref. [25] showed that local fluctuations in the boundary stress arise from a gap-spanning high-viscosity phase. Thus if the enhanced shear thickening in ULP and DP samples arises from an increase in contact networks, increased boundary stress fluctuations are expected as well.

We measured the local fluctuations in boundary stress for representative USP, ULP, and DP suspensions and quantified the average boundary stress as a function of time (Fig. 4). Whereas no significant heterogeneities in boundary stress were observed in any sample at low shear rates ($\dot{\gamma} \leq 100\ \text{s}^{-1}$), samples containing large PAM (ULP, DP) exhibited pronounced spatial heterogeneities in boundary stress in the shear-thickening regime (Fig. 4a). For $\dot{\gamma} = 100\ \text{s}^{-1}$, fluctuations in average boundary stress remained below 20 Pa (Fig. 4b). When the shear rate was increased ($\dot{\gamma} = 500\ \text{s}^{-1}$), USP exhibited more frequent fluctuations, but the magnitude remained low. Samples containing larger polymer, however, developed higher boundary stress fluctuations, with maxima of 89 Pa and 140 Pa in ULP and DP, respectively. The maximum fluctuation magnitudes were lower than those measured at higher ϕ in concentrated hard-sphere suspensions [25], for which more particles were in the contact network. The increases in magnitude and frequency of boundary stress heterogeneities in ULP/DP samples (compared to USP) are consistent with the idea that enhanced shear thickening in these samples results from transient, sample-spanning contact networks.

The data in Figs. 1–4 indicate that large polymers modify shear-thickening behavior in colloidal suspensions by inducing contact networks. The increase in contacts does not originate from stronger equilibrium depletion attractions, as the magnitude of the depletion attraction is greater for polymers with lower M_w at fixed c/c^* because of higher polymer number density and thus higher osmotic pressure [36–38].

The viscosity data do not show qualitative signatures of even weak, transient bridging of particles by polymers [17, 39]. All PAM solutions exhibited similar values of N_1 in the absence of particles, independent of PAM size [35]. This comparison suggests that the change in sign from N_1 does not arise from increasing contributions from polymer elasticity [18, 19, 40, 41] and that strain hardening of polymers due to elongational flow around the particles [21–23] does not drive shear thickening. Finally, measurements of $\phi = 0.45$ suspensions of poly(methyl methacrylate) particles in a dilute, viscous solution of large polystyrene ($M_w \approx 15$ MDa) also showed enhanced shear thickening and change in sign of N_1 from negative to positive compared to hard spheres. Thus, the elasticity of the polymer solution is not responsible for these rheological signatures in our system.

Instead, we posit that the lubrication layers break down [10, 32] when polymers are excluded by size from the gaps between particles, thereby promoting particle contacts. The quiescent radii of gyration of USP and ULP are ≈ 20 nm and 46 nm, respectively. To assess the effects of shear on polymer conformation, we calculate a Weissenberg number $\text{Wi} = \tau\dot{\gamma}$, where τ is the estimated polymer relaxation time. For suspensions with $c/c^* \approx 0.7$ at $\dot{\gamma} = 100\ \text{s}^{-1}$, $\text{Wi}_{\text{USP}} \approx 0.1$ and $\text{Wi}_{\text{ULP}} \approx 1.0$, suggesting that both polymers are partially extended [42]. The contour length of ULP is $\sim$4 μm, much larger than the average separation $d \approx 0.3\ \mu$m between particle surfaces at $\phi = 0.40$ estimated from geometric arguments [30]. Thus shear may drive exclusion of large polymers from the lubrication layers. By contrast, USP's contour length, $\sim 0.6\ \mu$m, is comparable to d. USP is therefore unlikely to be shear-excluded by size from between the particles. Indeed, USP and hard-sphere suspensions exhibit similar shear thickening and N_1, in accord with the idea that USP is small enough to remain entrained within lubrication layers.

This picture is consistent with experiments [43, 44] and theory/simulations [45, 46] on active microrheology, which show that very strong attractions can arise from non-equilibrium osmotic forces generated when depletants are excluded from gaps between particles. Size-dependent exclusion of polymers is also consistent with the lower $f_{\text{max}} \approx 0.8$ of DP: if the smaller polymers in

DP remain entrained in lubrication layers, fewer particles would be expected to make contact. Finally, our exclusion picture is consistent with the filled-polymer literature [18, 19, 40, 41], which states that N_1 is dominated by polymer elasticity and scales as a power-law with σ [19]. This scaling holds for ULP/DP suspensions when $N_1 > 0$, suggesting that polymers contribute independently to N_1 once excluded from interparticle gaps.

Our results suggest that large polymers promote particle contact networks that enhance CST and change sign of N_1 from negative to positive. Contact network formation represents an additional mechanism by which polymers can alter shear thickening of suspensions, enabling new routes to probe shear thickening. Microscopically, our results are consistent with exclusion of large polymers from lubrication layers, which allows particles to make contact. Insight into non-equilibrium interactions in flowing dense, particle/polymer mixtures is not attainable with current simulation capabilities, but may be accessible in experiments using labeled polymers. The ability to tailor polymer additives and thereby modulate the shear thickening response offers new opportunities in the design of complex materials for technology [47, 48].

We thank J. Palmer and N. Wagner for constructive discussions. This work was supported by the National Science Foundation (CBET-1803728) and the Welch Foundation (E-1869). N. P. acknowledges partial funding from the Houston Endowment Fund.

---

* Corresponding author.
jcconrad@uh.edu

[1] M. M. Denn, J. F. Morris, and D. Bonn, Soft Matter **14**, 170 (2018).
[2] T. N. Phung, J. F. Brady, and G. Bossis, J. Fluid Mech. **313**, 181 (1996).
[3] N. J. Wagner and J. F. Brady, Phys. Today **62**, 27 (2009).
[4] C. D. Cwalina and N. J. Wagner, J. Rheol. **58**, 949 (2014).
[5] M. Wyart and M. E. Cates, Phys. Rev. Lett. **112**, 098302 (2014).
[6] E. Brown and H. M. Jaeger, J. Rheol. **56**, 875 (2012).
[7] E. Brown and H. M. Jaeger, Rep. Prog. Phys. **77**, 046602 (2014).
[8] R. Mari, R. Seto, J. F. Morris, and M. M. Denn, J. Rheol. **58**, 1693 (2014).
[9] N. Y. C. Lin, B. M. Guy, M. Hermes, C. Ness, J. Sun, W. C. K. Poon, and I. Cohen, Phys. Rev. Lett. **115**, 228304 (2015).
[10] J. R. Royer, D. L. Blair, and S. D. Hudson, Phys. Rev. Lett. **116**, 188301 (2016).
[11] D. R. Foss and J. F. Brady, J. Fluid Mech. **407**, 167 (2000).
[12] J. Bergenholtz, J. F. Brady, and M. Vicic, J. Fluid Mech. **456**, 239 (2002).
[13] O. Reynolds, Lond. Edinb. Dubl. Phil. Mag. J. Sci. **20**, 469 (1885).
[14] V. Gopalakrishnan and C. F. Zukoski, J. Rheol. **48**, 1321 (2004).
[15] E. Brown, N. A. Forman, C. S. Orellana, H. Zhang, B. W. Maynor, D. E. Betts, J. M. DeSimone, and H. M. Jaeger, Nat. Mater. **9**, 220 (2010).
[16] S. Pednekar, J. Chun, and J. F. Morris, Soft Matter **13**, 1773 (2017).
[17] Y. Otsubo and K. Umeya, J Colloid Interface Sci. **95**, 279 (1983).
[18] I. E. Zarraga, D. A. Hill, and D. T. Leighton, J. Rheol. **45**, 1065 (2001).
[19] S. E. Mall-Gleissle, W. Gleissle, G. H. McKinley, and H. Buggisch, Rheol. Acta **41**, 61 (2002).
[20] B. A. Haleem and P. R. Nott, J. Rheol. **53**, 383 (2009).
[21] R. Scirocco, J. Vermant, and J. Mewis, J. Rheol. **49**, 551 (2005).
[22] M. Yang and E. S. G. Shaqfeh, J. Rheol. **62**, 1363 (2018).
[23] M. Yang and E. S. G. Shaqfeh, J. Rheol. **62**, 1379 (2018).
[24] B. M. Guy, M. Hermes, and W. C. K. Poon, Phys. Rev. Lett. **115**, 088304 (2015).
[25] V. Rathee, D. L. Blair, and J. S. Urbach, Proc. Natl. Acad. Sci. USA **114**, 8740 (2017).
[26] T. E. Kodger, R. E. Guerra, and J. Sprakel, Sci. Rep. **5**, 14635 (2015).
[27] N. Park, E. J. Umanzor, and J. C. Conrad, Front. Phys. **6**, 42 (2018).
[28] Selected measurements were verified on a DHR-3 rheometer (TA Instruments) with the same cone and an MCR-301 (Anton Paar USA, Ashland, VA) with 25 mm diameter, 1° stainless steel cone. Varying instrument and cone resulted in identical values of η and N_1 within sample-to-sample variability. A 40 mm parallel plate geometry with 1000 grit sandpaper (3M, St. Paul, MN) attached on both top and bottom surfaces was used to check for slip. The resulting η, when corrected for gap changes from surface roughness and radial dependence of stress in parallel plates [34], was the same as that measured using the smooth 40 mm diameter, 2° cone. These measurements confirmed that slip was insignificant in these samples, and that changes in shear thickening did not arise from elastic instabilities.
[29] W. M. Kulicke, G. Kiss, and R. S. Porter, Rheol. Acta **16**, 568 (1977).
[30] T. Chatterjee, A. K. Van Dyk, V. V. Ginzburg, and A. I. Nakatani, ACS Macro Lett. **6**, 716 (2017).
[31] R. M. Turian, Ind. Eng. Chem. Fundam. **11**, 361 (1972).
[32] L. C. Hsiao, S. Jamali, E. Glynos, P. F. Green, R. G. Larson, and M. J. Solomon, Phys. Rev. Lett. **119**, 158001 (2017).
[33] D. B. Genovese, Adv. Colloid Interface Sci. **171-172**, 1 (2012).
[34] J. Mewis and N. J. Wagner, Colloidal Suspension Rheology (Cambridge University Press, 2012).
[35] See Supplemental Material at [URL] for rheology of polymer solutions, discussion of fitting protocols to the model of Ref. [5], and comparisons to concentrated hard-sphere suspensions and filled polymer melts, which includes Refs. [49–51].
[36] S. Asakura and F. Oosawa, J. Polym. Sci. **33**, 183 (1958).
[37] S. M. Ilett, A. Orrock, W. C. K. Poon, and P. N. Pusey, Phys. Rev. E **51**, 1344 (1995).
[38] H. N. W. Lekkerkerker and R. Tuinier, Colloids and the depletion interaction (Springer Nether-

lands, 2011).
[39] Y. Otsubo, Chem. Eng. Sci. **56**, 2939 (2001).
[40] Y. Lin, N. Phan-Thien, and B. C. Khoo, J. Rheol. **58**, 223 (2014).
[41] Y. Lin, N. Phan-Thien, and B. C. Khoo, J. Non-Newton. Fluid Mech. **239**, 28 (2017).
[42] H. Chen and A. Alexander-Katz, Phys. Rev. Lett. **107**, 128301 (2011).
[43] I. Sriram and E. M. Furst, Soft Matter **8**, 3335 (2012).
[44] I. Sriram and E. M. Furst, Phys. Rev. E **91**, 042303 (2015).
[45] J. Dzubiella, H. Lwen, and C. N. Likos, Phys. Rev. Lett. **91**, 248301 (2003).
[46] R. Wulfert, U. Seifert, and T. Speck, Soft Matter **13**, 9093 (2017).
[47] Y. S. Lee, E. D. Wetzel, and N. J. Wagner, J. Mater. Sci. **38**, 2825 (2003).
[48] J. N. Fowler, A. A. Pallanta, C. B. Swanik, and N. J. Wagner, J. Biomech. Eng. **137**, 054504 (2015).
[49] M. E. Cates, J. P. Wittmer, J.-P. Bouchaud, and P. Claudin, Phys. Rev. Lett. **81**, 1841 (1998).
[50] Q. Tseng, E. Duchemin-Pelletier, A. Deshiere, M. Balland, H. Guillou, O. Filhol, and M. Thry, Proc. Natl. Acad. Sci. USA **109**, 1506 (2012).
[51] R. W. Style, R. Boltyanskiy, G. K. German, C. Hyland, C. W. MacMinn, A. F. Mertz, L. A. Wilen, Y. Xu, and E. R. Dufresne, Soft Matter **10**, 4047 (2014).